

TIME COUPLED DIFFUSION MAPS

NICHOLAS F. MARSHALL AND MATTHEW J. HIRN

ABSTRACT. We consider a collection of n points in \mathbb{R}^d measured at m times, which are encoded in an $n \times d \times m$ data tensor. Our objective is to define a single embedding of the n points into Euclidean space which summarizes the geometry as described by the data tensor. In the case of a fixed data set, diffusion maps and related graph Laplacian methods define such an embedding via the eigenfunctions of a diffusion operator constructed on the data. Given a sequence of m measurements of n points, we introduce the notion of time coupled diffusion maps which have natural geometric and probabilistic interpretations. To frame our method in the context of manifold learning, we model evolving data as samples from an underlying manifold with a time-dependent metric, and we describe a connection of our method to the heat equation on such a manifold.

1. INTRODUCTION

In many machine learning and signal processing tasks, the observable data is high dimensional, but it lies on a low-dimensional intrinsic manifold. In recent years, several manifold learning methods have emerged which attempt to recover the intrinsic manifold underlying datasets. In particular, graph Laplacian methods have become popular due to their practicality and theoretical guarantees [1, 2, 3, 4, 5, 6, 7, 8].

Current graph Laplacian methods implicitly assume a static intrinsic manifold, or equivalently, that the dynamics underlying the data generation process are stationary. For many applications, this stationary assumption is justified, as datasets often consist of a single snapshot of a system, or are recorded over small time windows. However, in the case where data is accumulated over longer periods of time, accounting for changing dynamics may be advantageous. Furthermore, if a system is particularly noisy, combining a large number of snapshots over time may help recover structure hidden in noise. These observations raise the following question: how can graph Laplacian methods be extended to account for changing dynamics while maintaining theoretical guarantees?

In this paper, we propose modeling data with changing dynamics by assuming there exists an underlying intrinsic manifold with a time-dependent metric. We will describe the proposed method using the diffusion maps framework: a popular graph Laplacian framework which is robust to non-uniform sampling [4]. We remark that diffusion maps are highly related to other manifold learning methods such as Laplacian eigenmaps and spectral clustering. In fact, if data is uniformly sampled from the underlying manifold, diffusion maps [4] is essentially eigenvalue weighted Laplacian eigenmaps [9].

Although we assume points on the intrinsic manifold are fixed, their geometry, i.e, dependence structure, is allowed change. We can conceptualize samples from a manifold with a time-dependent metric by considering a corresponding point cloud smoothly moving through \mathbb{R}^d produced by isometrically embedding the manifold over time. The evolution of the metric dictates the movement of points, and vice versa. In practice, datasets conforming to this model are commonly encountered, e.g., an RGB video feed consists of a collection of n pixels which move through \mathbb{R}^3 .

In general, we consider data consisting of a collection of n points in \mathbb{R}^d measured at m times encoded in an $n \times d \times m$ data tensor X . The tensor X can be expressed as a sequence (X_1, \dots, X_m) of $n \times d$ matrices whose entries correspond across the sequence. Given such a sequence (X_1, \dots, X_m) ,

Key words and phrases. Manifold learning; Dimensionality reduction; Diffusion distance; Heat equation; Time-dependent metric.

the time coupled diffusion map framework introduced in this paper is based on the product operator:

$$(1) \quad \mathbf{P}^{(m)} = \mathbf{P}_m \mathbf{P}_{m-1} \cdots \mathbf{P}_2 \mathbf{P}_1,$$

where each \mathbf{P}_i is a diffusion operator constructed from X_i . We will show that this discrete diffusion process, which is formally defined in the following section, approximates a continuous diffusion process on an assumed underlying manifold with a time-dependent metric. Additionally, we introduce the notion of time coupled diffusion maps, named thus because the time evolution of the data has been coupled to the time evolution of a diffusion process.

1.1. Related works. In the diffusion geometry literature, several techniques have been developed, which also utilize multiple diffusion kernels for a variety of objectives including: iteratively refining the representation of data, facilitating comparison, and combining multiple measurements of a fixed system.

An early example of a multiple kernel method is the denoising algorithm of Szlam, Maggioni, and Coifman [10], which iteratively smooths an image via an anisotropic diffusion process. That is, the algorithm switches between constructing a diffusion kernel on a given data set (in this case an image), and applying the constructed kernel to the data:

$$X_i \rightarrow \mathbf{P}_i, \quad X_{i+1} = \mathbf{P}_i X_i$$

where the arrow denotes that \mathbf{P}_i is constructed based on X_i . More recently, in [11] Welp, Wolf, Hirn, and Krishnaswamy introduce an iterative diffusion based construction, which acts to coarse grain data. From a theoretical perspective, both of these methods can be considered in the context of the time coupled diffusion framework introduced in this paper.

In [12] Wang, Jiang, Wang, Zhou, and Tu introduce the notion of Cross Diffusion as a metric fusion algorithm with applications to image processing. They demonstrate how multiple metrics on a given data set can be combined by considering the iterative cross diffusion

$$\mathbf{P}_1^{(t+1)} = \mathbf{P}_1 \mathbf{P}_2^{(t)} \mathbf{P}_1^T, \quad \text{and} \quad \mathbf{P}_2^{(t+1)} = \mathbf{P}_2 \mathbf{P}_1^{(t)} \mathbf{P}_2^T,$$

where $\mathbf{P}_1^{(0)} = \mathbf{P}_1$ and $\mathbf{P}_2^{(0)} = \mathbf{P}_2$ are constructed from two different metrics on the given data. A generalized method for m metrics is also described.

In [13] Coifman and Hirn present a method of extending diffusion maps to allow comparisons across multiple measurements of a system, even when such measurements are of different modalities.

In [14, 15] Lederman and Talmon introduce the idea of Alternating Diffusion: a method of combining measurements from multiple sensors to extract the common source of variability (i.e., the common manifold), while filtering out sensor specific effects. The method is based on the product operators

$$\mathbf{P}_1 \mathbf{P}_2, \quad \text{and} \quad \mathbf{P}_2 \mathbf{P}_1,$$

where \mathbf{P}_1 and \mathbf{P}_2 are constructed from two different views of the data. In [16], Lindenbaum, Yeredor, Salhov, and Averbuch follow a similar approach, but concatenate a collection of alternating products in block matrix defining Multi-View Diffusion Maps. Recently, several applications and extensions of Alternating Diffusion have been developed. In [15] Lederman, Talmon, Wu, Lo, and Coifman demonstrate an application of Alternating Diffusion to sleep stage assessment. In [17] Talmon and Wu describe a general notion of nonlinear manifold filtering, which extracts a common manifold from multiple sensors.

Our work extends the current diffusion maps literature by considering evolving dynamics rather than enhancing the analysis of a fixed system. We consider an $n \times d \times m$ data tensor describing a system of n points in \mathbb{R}^d over m times, and seek to construct a manifold model and diffusion geometry framework for this setting. A similar framework is considered by Banisch and Koltai in [18]. However, rather than study the product operator (1), they study the sum of the operators \mathbf{P}_i and prove a relation with the dynamic Laplacian.

1.2. Organization. The remainder of the paper is organized as follows. In Section 2 we describe the construction of time coupled diffusion maps. In Section 3 we establish a connection between the product operator $\mathbf{P}^{(t)}$ and the heat kernel on the assumed underlying manifold with a time-dependent metric. In Section 4 we present numerical results on synthetic data. Section 5 investigates the continuous analog of the operator $\mathbf{P}^{(t)}$ and the corresponding time coupled diffusion distance. Concluding remarks are given in Section 6.

2. TIME COUPLED DIFFUSION MAPS

In this section, we introduce the notion of time coupled diffusion maps.

2.1. Notation. Let \mathcal{M} be a compact smooth manifold with a smooth 1-parameter family of Riemannian metrics $g(\tau)$, $\tau \in [0, T]$, $T < \infty$. We refer to the parameter τ as time throughout. For each time τ , let $\iota_\tau : \mathcal{M} \hookrightarrow \mathbb{R}^d$, $\mathcal{M}_\tau = \iota_\tau(\mathcal{M})$, denote an isometric embedding of $(\mathcal{M}, g(\tau))$ into d -dimensional Euclidean space, where d is fixed for all $\tau \in [0, T]$. Let $X = \{x_j\}_{j=1}^n \subseteq \mathcal{M}$ denote a finite collection of n points sampled from \mathcal{M} and let $(\tau_0, \tau_1, \dots, \tau_m)$ be a uniform partition of $[0, T]$ with $\tau_0 = 0$ and $\tau_m = T$. We assume that our data consists of measurements of the n points X at times τ_1, \dots, τ_m such that we have one measurement set for each of the time intervals $(\tau_{i-1}, \tau_i]$ for $i = 1, \dots, m$. More precisely, our data will consist of a sequence of m sets (X_1, \dots, X_m) , where $X_i = \iota_{\tau_i}(X) = \{x_j^{(i)}\}_{j=1}^n$; see Figure 1 for an illustration.

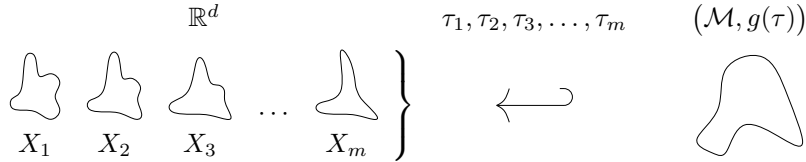


FIGURE 1. Illustration of the data model

Such data can be represented as an $n \times d \times m$ tensor corresponding to n points in \mathbb{R}^d measured at m times. Suppose each X_i is distributed over \mathcal{M}_{τ_i} according to a density $q_{\tau_i} : \mathcal{M}_{\tau_i} \rightarrow \mathbb{R}$. We assume that at time τ_1 , the n points $X_1 = \{x_j^{(1)}\}_{j=1}^n$ are sampled independently from \mathcal{M}_{τ_1} according to the density q_{τ_1} . Since no re-sampling occurs, any changes in the densities q_{τ_i} , for $i = 1, \dots, m$, result from deformations of q_{τ_1} induced by changes in the Riemannian volume of \mathcal{M} , which itself is induced from changes in the Riemannian metric $g(\tau)$ over time. In particular, $x_j^{(i)} = \iota_{\tau_i} \circ \iota_{\tau_1}^{-1}(x_j^{(1)})$ and $q_{\tau_i}(x) = q_{\tau_1}(\iota_{\tau_1} \circ \iota_{\tau_i}^{-1}(x)) |\det(D(\iota_{\tau_1} \circ \iota_{\tau_i}^{-1}))(x)|$.

Remark. *Two remarks are in order.*

- (1) *Even if the initial sampling density is uniform, the changing geometry may alter the density over time. Hence, the density invariant kernel construction described in [2, 4] plays an essential role in our construction. We assume the minimum sampling density over time is bounded below and the associated error term enters our analysis as a constant. We refer the reader to a recent paper by Berry and Harlim [19] for a detailed error analysis of variable density kernel constructions.*
- (2) *Since we have assumed the initial samples X_1 are i.i.d., then for fixed i , each set of samples X_i are also i.i.d since X_i is the continuous, hence measurable, function $\iota_{\tau_i} \circ \iota_{\tau_1}^{-1}$ of the i.i.d. variables X_1 .*

2.2. Kernel construction. Given a sequence of data sets (X_1, \dots, X_m) as described above, we proceed as follows. For each data set X_i , we construct a diffusion operator $\mathbf{P}_{\varepsilon, i}$ following the diffusion maps framework [4]. For completeness, we include the details of the construction of $\mathbf{P}_{\varepsilon, i}$ in the following. For each time index i , we define a Gaussian kernel $\mathbf{K}_{\varepsilon, i}$ on X using the measurements X_i ,

$$(2) \quad \mathbf{K}_{\varepsilon, i}(x_j, x_k) = \exp\left(-\frac{\|x_j^{(i)} - x_k^{(i)}\|_2^2}{4\varepsilon}\right), \quad x_j, x_k \in X \text{ and } x_j^{(i)}, x_k^{(i)} \in X_i,$$

where $\|\cdot\|_2$ denotes the Euclidean norm in the ambient space \mathbb{R}^d . By summing over the second variable of the kernel $\mathbf{K}_{\varepsilon,i}$ we approximate the density q_{τ_i} by

$$(3) \quad \mathbf{q}_{\varepsilon,i}(x_j) = \sum_{k=1}^n \mathbf{K}_{\varepsilon,i}(x_j, x_k), \quad x_j \in X.$$

Using $\mathbf{q}_{\varepsilon,i}$ we normalize the kernel $\mathbf{K}_{\varepsilon,i}$ as follows

$$(4) \quad \tilde{\mathbf{K}}_{\varepsilon,i}(x_j, x_k) = \frac{\mathbf{K}_{\varepsilon,i}(x_j, x_k)}{\mathbf{q}_{\varepsilon,i}(x_j)\mathbf{q}_{\varepsilon,i}(x_k)}, \quad x_j, x_k \in X.$$

Then the corresponding diffusion operator $\mathbf{P}_{\varepsilon,i} : \mathbb{R}^n \rightarrow \mathbb{R}^n$ is given by

$$(5) \quad (\mathbf{P}_{\varepsilon,i}f)(x_j) = \sum_{k=1}^n \frac{\tilde{\mathbf{K}}_{\varepsilon,i}(x_j, x_k)}{\sum_{l=1}^n \tilde{\mathbf{K}}_{\varepsilon,i}(x_j, x_l)} f(x_k).$$

Each $\mathbf{P}_{\varepsilon,i}$ is a matrix which is a diffusion operator when applied to column vectors on the left, and a Markov operator when applied row vectors on the right. For $1 \leq t \leq m$, define:

$$(6) \quad \mathbf{P}_{\varepsilon}^{(t)} = \mathbf{P}_{\varepsilon,t} \mathbf{P}_{\varepsilon,t-1} \cdots \mathbf{P}_{\varepsilon,1}.$$

Like its constituent components, the matrix $\mathbf{P}_{\varepsilon}^{(t)}$ is a diffusion operator when acting on column vectors from the left and a Markov operator when acting on row vectors from the right. As a Markov operator, $\mathbf{P}_{\varepsilon}^{(t)}$ acts backwards in time, in the sense that $\mathbf{P}_{\varepsilon}^{(t)}$ acts by first applying $\mathbf{P}_{\varepsilon,t}$, second $\mathbf{P}_{\varepsilon,t-1}$ and so on. On the other hand, as a diffusion operator $\mathbf{P}_{\varepsilon}^{(t)}$ acts forward in time, first applying $\mathbf{P}_{\varepsilon,1}$, second applying $\mathbf{P}_{\varepsilon,2}$ and so on. We have chosen the ordering convention in equation (6) to favor the geometric interpretation.

2.3. Time coupled diffusion distance. Let δ_j denote a Dirac distribution centered at x_j , i.e., $\delta_j(x_j) = 1$ and $\delta_j = 0$ elsewhere. We compare the points x_j and x_k by comparing the posterior distributions of δ_j^T and δ_k^T under the Markov operator $\mathbf{P}_{\varepsilon}^{(t)}$. More specifically, following [4] we define a diffusion based distance as the L^2 distance between these posterior distributions weighted by the reciprocal of the stationary distribution of the Markov chain. That is, we define the distance $D_{\varepsilon}^{(t)}$ by

$$(7) \quad D_{\varepsilon}^{(t)}(x_j, x_k) = \|\delta_j^T \mathbf{P}_{\varepsilon}^{(t)} - \delta_k^T \mathbf{P}_{\varepsilon}^{(t)}\|_{L^2(1/\pi_{(t)})},$$

where $\pi_{(t)}$ is the stationary distribution of $\mathbf{P}_{\varepsilon}^{(t)}$, i.e., $\pi_{(t)}^T \mathbf{P}_{\varepsilon}^{(t)} = \pi_{(t)}^T$, and $\|\cdot\|_{L^2(1/\pi_{(t)})}$ is the weighted L^2 norm:

$$(8) \quad \|\mathbf{f}\|_{L^2(1/\pi_{(t)})} := \sqrt{\sum_{j=1}^n \mathbf{f}(x_j)^2 \frac{1}{\pi_{(t)}(x_j)}}.$$

We refer to $D_{\varepsilon}^{(t)}$ as the *time coupled diffusion distance*, since it extends the diffusion distance in [4] by coupling the evolution time of the data (X_1, \dots, X_t) with that of the diffusion process governed by $(\mathbf{P}_{\varepsilon,1}, \dots, \mathbf{P}_{\varepsilon,t})$. Our next objective is to construct a *time coupled diffusion map*, that is, an embedding of X into Euclidean space which preserves the time coupled diffusion distance. For notational brevity, we suppress the dependence on ε in the following.

2.4. Time coupled diffusion map. Recall that the diffusion map for a static manifold (\mathcal{M}, g) is defined in terms of the eigenvectors and eigenvalues of the transition matrix \mathbf{P} , which is constructed in the same manner as (5). The inhomogeneous transition operator $\mathbf{P}^{(t)}$ is also row stochastic, but unlike \mathbf{P} , does not necessarily have a complete basis of real eigenvectors. Instead, we define the operator $\mathbf{A}^{(t)}$ by

$$(9) \quad \mathbf{A}^{(t)} = \mathbf{\Pi}_{(t)}^{1/2} \mathbf{P}^{(t)} \mathbf{\Pi}_{(t)}^{-1/2},$$

where $\mathbf{\Pi}_{(t)}$ denotes the matrix with the stationary distribution $\pi_{(t)}$ of $\mathbf{P}^{(t)}$ along the diagonal and zeros elsewhere. First, observe that $\pi_{(t)}^{1/2}$ is both a right and left eigenvector of $\mathbf{A}^{(t)}$ with eigenvalue

1. In fact, $\mathbf{A}^{(t)}$ has operator norm one and naturally arises when constructing a diffusion framework starting with a Markov chain, see A. Next, we compute the singular value decomposition (SVD) of $\mathbf{A}^{(t)}$:

$$(10) \quad \mathbf{A}^{(t)} = \mathbf{U}_{(t)} \boldsymbol{\Sigma}_{(t)} \mathbf{V}_{(t)}^T,$$

where $\mathbf{U}_{(t)}$ is an orthogonal matrix of left singular vectors, $\boldsymbol{\Sigma}_{(t)}$ is a diagonal matrix of corresponding singular values, and $\mathbf{V}_{(t)}$ is an orthogonal matrix of right singular vectors. Define

$$(11) \quad \boldsymbol{\Psi}^{(t)} := \boldsymbol{\Pi}_{(t)}^{-1/2} \mathbf{U}_{(t)} \boldsymbol{\Sigma}_{(t)}.$$

Lemma 2.1. *The embedding*

$$(12) \quad x_j \mapsto \delta_j^T \boldsymbol{\Psi}^{(t)}$$

of the data X into Euclidean space preserves the time coupled diffusion distance. That is to say,

$$D^{(t)}(x_j, x_k) = \|\delta_j^T \boldsymbol{\Psi}^{(t)} - \delta_k^T \boldsymbol{\Psi}^{(t)}\|_{L^2}.$$

We refer to the embedding $x_j \mapsto \delta_j^T \boldsymbol{\Psi}^{(t)}$ as the time coupled diffusion map.

Proof. By the definition of time coupled diffusion distance (7), and by definition of the weighted L^2 norm (8)

$$(13) \quad D^{(t)}(x_j, x_k) = \|\delta_j^T \mathbf{P}^{(t)} - \delta_k^T \mathbf{P}^{(t)}\|_{L^2(1/\pi_{(t)})} = \|\delta_j^T \mathbf{P}^{(t)} \boldsymbol{\Pi}^{-1/2} - \delta_k^T \mathbf{P}^{(t)} \boldsymbol{\Pi}^{-1/2}\|_{L^2}.$$

Multiplying equation (9) by $\boldsymbol{\Pi}_{(t)}^{-1/2}$ yields

$$\boldsymbol{\Pi}_{(t)}^{-1/2} \mathbf{A}^{(t)} = \mathbf{P}^{(t)} \boldsymbol{\Pi}_{(t)}^{-1/2},$$

and substituting this expression into (13) gives

$$D^{(t)}(x_j, x_k) = \|\delta_j^T \boldsymbol{\Pi}_{(t)}^{-1/2} \mathbf{A}^{(t)} - \delta_k^T \boldsymbol{\Pi}_{(t)}^{-1/2} \mathbf{A}^{(t)}\|_{L^2}.$$

Expanding $\mathbf{A}^{(t)}$ in its singular value decomposition (10) yields,

$$D^{(t)}(x_j, x_k) = \|\delta_j^T \boldsymbol{\Pi}_{(t)}^{-1/2} \mathbf{U}_{(t)} \boldsymbol{\Sigma}_{(t)} \mathbf{V}_{(t)}^T - \delta_k^T \boldsymbol{\Pi}_{(t)}^{-1/2} \mathbf{U}_{(t)} \boldsymbol{\Sigma}_{(t)} \mathbf{V}_{(t)}^T\|_{L^2}.$$

Now, since the transformation $\mathbf{V}_{(t)}$ is orthogonal,

$$D^{(t)}(x_j, x_k) = \|\delta_j^T \boldsymbol{\Pi}_{(t)}^{-1/2} \mathbf{U}_{(t)} \boldsymbol{\Sigma}_{(t)} - \delta_k^T \boldsymbol{\Pi}_{(t)}^{-1/2} \mathbf{U}_{(t)} \boldsymbol{\Sigma}_{(t)}\|_{L^2},$$

and substituting $\boldsymbol{\Psi}^{(t)} = \boldsymbol{\Pi}_{(t)}^{-1/2} \mathbf{U}_{(t)} \boldsymbol{\Sigma}_{(t)}$ into this equation yields the result. \square

Remark. *Several remarks regarding time coupled diffusion maps are in order.*

- (1) *If $t = 1$, the time coupled diffusion map (12) is equivalent to the definition of the standard density invariant diffusion map in [4], see the calculations in A, which are motivated by similar calculations in [2].*
- (2) *The first coordinate of the embedding (12) is always constant because $\pi_{(t)}^{1/2}$ is the top left singular vector of $\mathbf{A}^{(t)}$, and therefore, this coordinate of the embedding can be discarded.*
- (3) *In order to produce an embedding of X into \mathbb{R}^l for some $l > 0$, we can compute a rank $l + 1$ singular value decomposition in equation (10) and map*

$$x_j \mapsto \delta_j^T \boldsymbol{\Psi}_l^{(t)},$$

where $\boldsymbol{\Psi}_l^{(t)}$ denotes the matrix consisting of columns 2 through $l + 1$ of the matrix $\boldsymbol{\Psi}^{(t)}$. Since the singular values of $\mathbf{A}^{(t)}$ are of the form $1 = \sigma_0 > \sigma_1 \geq \dots \geq \sigma_{n-1}$, the truncated embedding will preserve the diffusion distance up to an error on the order of σ_{l+1} . As in other diffusion based methods, in the case where data lies on a low dimensional manifold, we expect the first few coordinates of the embedding to provide a meaningful summary of the data.

2.5. Comparison to standard diffusion maps. It is instructive at this point to make a comparison with the original diffusion maps of Coifman and Lafon [4]. In that setting, one is given samples X of an isometric embedding of a manifold \mathcal{M} with a *static* metric g . The density invariant version of diffusion maps uses the same construction as outlined in equations (2), (3), (4), and (5), which yields a Markov matrix \mathbf{P} , which is not indexed by a time i since the metric is static. Running this homogeneous Markov chain forward t steps is equivalent to composing \mathbf{P} with itself t times, i.e., \mathbf{P}^t . Since \mathbf{P} is, by construction, similar to a symmetric matrix, it can be decomposed into a diagonal matrix of real eigenvalues $\mathbf{\Lambda}$ and a basis of right eigenvectors $\mathbf{\Phi}$. Since the left eigenvectors of \mathbf{P} are orthogonal in $L^2(1/\pi)$, the diffusion map

$$(14) \quad x_j \mapsto \delta_j^T \mathbf{\Phi} \mathbf{\Lambda}^t,$$

preserves the diffusion distance $D^t(x_j, x_k) = \|\delta_j^T \mathbf{P}^t - \delta_k^T \mathbf{P}^t\|_{L^2(1/\pi)}$, where π is the stationary distribution of \mathbf{P} . A main result of [4] is that as $n \rightarrow \infty$ and $\varepsilon \rightarrow 0$, we have $\mathbf{P}_\varepsilon^{t/\varepsilon} \rightarrow e^{t\Delta}$, where $e^{t\Delta}$ is the Neumann heat kernel on \mathcal{M} . Since the eigenfunctions and eigenvalues of $e^{t\Delta}$ give a complete geometric description of the manifold \mathcal{M} [20], the diffusion maps embedding (14) learns the geometry of the manifold from the samples X .

In the time-dependent case, we consider a sequence of data (X_1, \dots, X_t) and construct a corresponding family of operators $(\mathbf{P}_1, \dots, \mathbf{P}_t)$. Rather than raising a matrix to a power, we compose the family of operators, obtaining $\mathbf{P}^{(t)}$ defined in equation (6). After defining a distance $D^{(t)}$ based on $\mathbf{P}^{(t)}$ we seek a distance preserving embedding. However, since the product of symmetric matrices is not in general symmetric, there is no reason we should suspect $\mathbf{P}^{(t)}$ to have a basis of real eigenvalues and eigenvectors. Therefore, we construct a diffusion maps framework based on the Markov operator using the singular value decomposition of the operator $\mathbf{A}^{(t)}$ as described in equations (9), (10), (11), and (12). We expect the operator $\mathbf{P}^{(t)}$ encodes some average sense of affinity across the data, and by extension that the time coupled diffusion map is similarly meaningful. In the following, we make the connection of $\mathbf{P}^{(t)}$ to the data precise by showing that $\mathbf{P}^{(t)}$ approximates the heat kernel on the underlying manifold $(\mathcal{M}, g(\cdot))$, which will be defined in Section 3. Thus, we conjecture that the time coupled diffusion map aggregates important geometrical information of the manifold $(\mathcal{M}, g(\cdot))$ over the time interval $[0, T]$. Numerical results in Section 4 lend credence to this conjecture. There is, however, no theoretical result that directly links geometrical information of $(\mathcal{M}, g(\cdot))$ over arbitrarily long time scales with its heat kernel. The closest results are contained in [21, 22], in which the heat kernel of $(\mathcal{M}, g(\cdot))$ is used to embed the manifold into a single Hilbert space, so that one can observe the flow of \mathcal{M} over time. This result, however, only holds for short time scales.

Before describing the connection of $\mathbf{P}^{(t)}$ to heat flow, we make a brief computational note. In practice, it is common to construct each diffusion matrix \mathbf{P}_i defined in equation (5) as a sparse matrix by, for example, truncating values which fall below a certain threshold. However, if the product

$$\mathbf{P}^{(t)} = \mathbf{P}_t \mathbf{P}_{t-1} \cdots \mathbf{P}_2 \mathbf{P}_1$$

is computed explicitly, there is no reason to expect sparsity will be maintained. Moreover, since each \mathbf{P}_i is a diffusion operator on an assumed underlying k -dimensional manifold \mathcal{M} , if each \mathbf{P}_i initially has l nonzero entries in each row, the number of nonzero entries in each row of the product $\mathbf{P}^{(t)}$ could be on the order of $(l \cdot t)^k$. Therefore, rather than explicitly constructing $\mathbf{P}^{(t)}$, we can treat $\mathbf{P}^{(t)}$ as an operator that can be applied to vectors in order $n \cdot l \cdot t$ operations. Using this approach, the singular value decomposition in equation (10) can be computed by iterative methods such as Lancroz iteration or subspace iteration [23]. When $n^2 > n \cdot l \cdot t$ this approach may provide significant computational savings, and reduce the memory requirements of the computation.

3. THE HEAT KERNEL FOR $(\mathcal{M}, g(\cdot))$

We begin by stating the definition and properties of the heat kernel for a manifold with time-dependent metric. Let $g(\tau), \tau \in [0, T]$, be a smooth family of metrics on a manifold \mathcal{M} . The heat

equation for such a manifold is:

$$(15) \quad \frac{\partial u}{\partial t} = \Delta_{g(t)} u,$$

where $u : \mathcal{M} \times [0, T] \rightarrow \mathbb{R}$. We say that

$$Z : (\mathcal{M} \times [0, T]) \times (\mathcal{M} \times [0, T]) \rightarrow \mathbb{R},$$

is the *heat kernel* for $\frac{\partial}{\partial t} - \Delta_{g(t)}$ if the following three conditions hold:

- (H₁) $Z(x, \tau; y, \sigma)$ is C^2 in the spacial variables x, y and C^1 in the temporal variables τ, σ ,
- (H₂) $(\frac{\partial}{\partial t} - \Delta_{g(t)}) Z(\cdot, \cdot; y, \sigma) = 0$, and
- (H₃) $\lim_{\tau \searrow \sigma} Z(\cdot, \tau; y, \sigma) = \delta_y$.

Several researchers have studied the heat equation (15) and corresponding heat kernel for a manifold $(\mathcal{M}, g(\cdot))$, in large part due to its relationship with the Ricci flow [24, 25], but also for data analysis [21]. The following properties of the heat kernel have been established (see [24]). First, the heat kernel exists and is the unique positive function satisfying (H₁), (H₂), and (H₃). Additionally, the solution to the initial value problem,

$$(16) \quad \begin{cases} \partial u / \partial t &= \Delta_{g(t)} u, \\ u(x, 0) &= f(x), \end{cases}$$

has the integral representation [24, Corollary 2.2]:

$$u(x, \tau) = \int_{\mathcal{M}} Z(x, \tau; y, 0) f(y) dV(y, 0),$$

where $V(\tau)$ is the Riemannian volume of \mathcal{M} at time τ . The heat kernel $Z(x, \tau; y, \sigma)$ also possesses properties analogous to those of the standard heat kernel, such as the semigroup property,

$$(17) \quad Z(x, \tau; y, \sigma) = \int_{\mathcal{M}} Z(x, \tau; \xi, \nu) Z(\xi, \nu; y, \sigma) dV(\xi, \nu), \quad \forall x, y \in \mathcal{M}, \nu \in (\sigma, \tau).$$

Furthermore, its ‘‘rows’’ sum to one, precisely stated as

$$(18) \quad \int_{\mathcal{M}} Z(x, \tau; y, \sigma) dV(y, \sigma) = 1, \quad \forall x \in \mathcal{M}, \sigma < \tau \in [0, T].$$

In the case of a static metric, the associated integral transform of the Neumann heat kernel is known to have the asymptotic approximation [4]:

$$(19) \quad e^{t\Delta} = \lim_{\varepsilon \rightarrow 0} (I + \varepsilon\Delta)^{t/\varepsilon} = (1 + \varepsilon\Delta)^{t/\varepsilon} + \mathcal{O}(\varepsilon).$$

For $t \leq T$, we define the associated integral transform of Z as the operator $T_Z^{(t)} : L^2(\mathcal{M}) \rightarrow L^2(\mathcal{M})$,

$$(20) \quad T_Z^{(t)} f(x) = \int_{\mathcal{M}} Z(x, t; y, 0) f(y) dV(y, 0).$$

We want to express $T_Z^{(t)}$ in an analogous form to (19); we would expect it to resemble $e^{\int_0^t \Delta_{g(\tau)} d\tau}$. However, as the family $\Delta_{g(\tau)}$ is not in general commutative with respect to composition, it is necessary to consider the *ordered exponential* of $\Delta_{g(\tau)}$ over $[0, t]$, which is the equivalent of the exponential for non-commutative operators, and which is denoted $\mathcal{T} e^{\int_0^t \Delta_{g(\tau)} d\tau}$. The ordered exponential can be expressed in terms of the power series:

$$\begin{aligned} \mathcal{T} e^{\int_0^t \Delta_{g(\tau)} d\tau} &= I + \int_0^t \Delta_{g(\tau)} d\tau + \int_0^t \Delta_{g(\tau)} \int_0^\tau \Delta_{g(\tau_1)} d\tau_1 d\tau + \dots \\ &= I + \sum_{i=1}^{\infty} \int_0^t \Delta_{g(\tau_1)} \int_0^{\tau_1} \Delta_{g(\tau_2)} \int_0^{\tau_2} \dots \int_0^{\tau_{i-2}} \Delta_{g(\tau_{i-1})} \int_0^{\tau_{i-1}} \Delta_{g(\tau_i)} d\tau_i d\tau_{i-1} \dots d\tau_2 d\tau_1, \end{aligned}$$

where I denotes the identity in the appropriate space. The operator \mathcal{T} can be thought of as enforcing time order in the products for the standard exponential expansion in a sense which is equivalent to the power series definition, cf. [26]. Considering $\mathcal{T} e^{\int_0^t \Delta_{g(\tau)} d\tau}$ as a formal power

series, it is easy to see that the heat equation is satisfied. Let $\{\phi_l\}_{l \geq 0}$ be the eigenfunctions of $\Delta_{g(0)}$, ordered in terms of increasing eigenvalue, and define $E_K := \text{Span}\{\phi_l : 0 \leq l \leq K\}$. Then $\Delta_{g(0)}$ is bounded on E_K , and furthermore as $g(\tau)$ is a smooth family of metrics for $\tau \in [0, T]$, we can conclude $\Delta_{g(\tau)}$ is uniformly bounded on E_K for all $\tau \in [0, T]$ (see B). Hence on E_K the power series for $\mathcal{T}e^{\int_0^t \Delta_{g(\tau)} d\tau}$ converges and by uniqueness we conclude $\mathcal{T}e^{\int_0^t \Delta_{g(\tau)} d\tau}$ is the heat kernel on E_K . Henceforth we will use

$$(21) \quad T_Z^{(t)} = \mathcal{T}e^{\int_0^t \Delta_{g(\tau)} d\tau}$$

as the notation for the Neumann heat kernel. We remark that E_K could also be defined independent of the differential structure of the manifold as K -band-limited functions on \mathcal{M} , cf. [27]. We prefer the former definition as it provides consistency with the definitions in [4].

Recall that n is the number of spatial samples of the manifold \mathcal{M} , and that m is the number of temporal measurements on the time interval $[0, T]$. We assume that the time interval $[0, T]$ is divided into m intervals $[\tau_{i-1}, \tau_i]$ each of length ε where $\tau_0 = 0$ and $\tau_m = T$. For simplicity, we assume that our m measurements are taken at (τ_1, \dots, τ_m) . Our main result is that in the limit of large data, both spatially and temporally, the transition operator $\mathbf{P}_\varepsilon^{(\lceil t/\varepsilon \rceil)}$ converges to the heat kernel:

$$\mathbf{P}_\varepsilon^{(\lceil t/\varepsilon \rceil)} \rightarrow \mathcal{T}e^{\int_0^t \Delta_{g(\tau)} d\tau} \text{ as } n \rightarrow \infty \text{ and } \varepsilon \rightarrow 0.$$

More precisely:

Theorem 3.1. *Suppose the isometric embedding $\mathcal{M}_\tau \subset \mathbb{R}^d$ of a time-dependent manifold $(\mathcal{M}, g(\tau))$ is measured at a common set $X = \{x_j\}_{j=1}^n \subset \mathcal{M}$ of n points at ε spaced units of time over a time interval $[0, T]$, so that, in particular, we have time samples $(\tau_i)_{i=1}^m \subset [0, T]$ with $\tau_i = i \cdot \varepsilon$ and $m = T/\varepsilon$.*

Then, for any sufficiently smooth function $f : \mathcal{M} \rightarrow \mathbb{R}$ and $t \leq T$, the heat kernel $\mathcal{T}e^{\int_0^t \Delta_{g(\tau)} d\tau}$ can be approximated by the operator $\mathbf{P}_\varepsilon^{(\lceil t/\varepsilon \rceil)}$:

$$(22) \quad \mathbf{P}_\varepsilon^{(\lceil t/\varepsilon \rceil)} f(x_j) = \mathcal{T}e^{\int_0^t \Delta_{g(\tau)} d\tau} f(x_j) + \mathcal{O}\left(\frac{1}{n^{1/2} \varepsilon^{d/4 + 1/2}}, \varepsilon\right), \quad x_j \in X.$$

We prove Theorem 3.1 in the following. Recall that E_K is defined to be the span for the first $K + 1$ eigenfunctions of the Laplace-Beltrami operator $\Delta_{g(0)}$.

Lemma 3.2. *On E_K , the heat kernel $\mathcal{T}e^{\int_\sigma^{\sigma+\varepsilon} \Delta_{g(\tau)} d\tau}$ admits the following asymptotic expansion:*

$$(23) \quad \mathcal{T}e^{\int_\sigma^{\sigma+\varepsilon} \Delta_{g(\tau)} d\tau} = I + \varepsilon \cdot \Delta_{g(\sigma)} + \mathcal{O}(\varepsilon^2).$$

Proof. By definition

$$I + \int_\sigma^{\sigma+\varepsilon} \Delta_{g(\tau)} d\tau + \int_\sigma^{\sigma+\varepsilon} \Delta_{g(\tau)} \int_\sigma^\tau \Delta_{g(\tau_1)} d\tau_1 d\tau + \int_\sigma^{\sigma+\varepsilon} \Delta_{g(\tau)} \int_\sigma^\tau \Delta_{g(\tau_1)} \int_\sigma^{\tau_1} \Delta_{g(\tau_2)} d\tau_2 d\tau_1 d\tau + \dots$$

The tail of this series starting with the third term is $\mathcal{O}(\varepsilon^2)$. For the second term, we can separate the contribution of $\Delta_{g(\sigma)}$ from the integral yielding:

$$\mathcal{T}e^{\int_\sigma^{\sigma+\varepsilon} \Delta_{g(\tau)} d\tau} = I + \varepsilon \cdot \Delta_{g(\sigma)} + \int_\sigma^{\sigma+\varepsilon} (\Delta_{g(\tau)} - \Delta_{g(\sigma)}) d\tau + \mathcal{O}(\varepsilon^2).$$

Now we can bound the integral by using the smoothness of $\Delta_{g(\tau)}$, which results from the smoothness of $g(\tau)$. By the smoothness of $\Delta_{g(\tau)}$ with respect to time and the fact that it is uniformly bounded on E_K for all $\tau \in [0, T]$,

$$\|\Delta_{g(\tau)} - \Delta_{g(\tau')}\| \leq C|\tau - \tau'|, \quad C \in \mathbb{R}^+.$$

Therefore,

$$\left| \int_\sigma^{\sigma+\varepsilon} (\Delta_{g(\tau)} - \Delta_{g(\sigma)}) d\tau \right| \leq \varepsilon \cdot \sup_{\tau \in [\sigma, \sigma+\varepsilon]} \|\Delta_{g(\tau)} - \Delta_{g(\sigma)}\| \leq C\varepsilon^2,$$

and hence we have:

$$\mathcal{T}e^{\int_\sigma^{\sigma+\varepsilon} \Delta_{g(\tau)} d\tau} = I + \varepsilon \cdot \Delta_{g(\sigma)} + \mathcal{O}(\varepsilon^2),$$

as desired. \square

By using the short time expansion from (23), we can develop a long time asymptotic expansion of the heat kernel. In the following, we write $\Delta_i = \Delta_{g(\tau_i)}$ to simplify notation.

Lemma 3.3. *Let $(\tau_0, \tau_1, \dots, \tau_m)$ be a uniform partition of $[0, T]$ with step size $\varepsilon > 0$, so that $\tau_i = \varepsilon \cdot i$ and $\tau_m = m \cdot \varepsilon = T$. For $0 < t \leq T$, define $\ell := \min_i \{i = 1, \dots, m \mid \tau_i \geq t\}$. Then on E_K the heat kernel $\mathcal{T}e^{\int_0^t \Delta_{g(\tau)} d\tau}$ has the expansion*

$$(24) \quad \mathcal{T}e^{\int_0^t \Delta_{g(\tau)} d\tau} = (I + \varepsilon \Delta_\ell) (I + \varepsilon \Delta_{\ell-1}) \cdots (I + \varepsilon \Delta_1) + \mathcal{O}(\varepsilon).$$

Proof. First suppose $t = \tau_\ell$. Using the semigroup property (17) of the heat kernel, we have:

$$(25) \quad \mathcal{T}e^{\int_0^t \Delta_{g(\tau)} d\tau} = \mathcal{T}e^{\int_{\tau_{\ell-1}}^{\tau_\ell} \Delta_{g(\tau)} d\tau} \cdot \mathcal{T}e^{\int_{\tau_{\ell-2}}^{\tau_{\ell-1}} \Delta_{g(\tau)} d\tau} \cdots \mathcal{T}e^{\int_{\tau_0}^{\tau_1} \Delta_{g(\tau)} d\tau}.$$

Combining the expansion (25) and Lemma 3.2, yields the following:

$$\begin{aligned} \mathcal{T}e^{\int_0^t \Delta_{g(\tau)} d\tau} &= (I + \varepsilon \Delta_\ell + \mathcal{O}(\varepsilon^2)) (I + \varepsilon \Delta_{\ell-1} + \mathcal{O}(\varepsilon^2)) \cdots (I + \varepsilon \Delta_1 + \mathcal{O}(\varepsilon^2)), \\ &= (I + \varepsilon \Delta_\ell) (I + \varepsilon \Delta_{\ell-1}) \cdots (I + \varepsilon \Delta_1) + \Xi. \end{aligned}$$

We now analyze the error term Ξ . First note that for small enough ε we have:

$$\|I + \varepsilon \Delta_i\| \leq 1, \quad \text{for all } i = 1, \dots, m.$$

Furthermore, since $[0, T]$ is fixed, the number of temporal measurements m is $m = T/\varepsilon = \mathcal{O}(1/\varepsilon)$. Putting together these two facts, one obtains:

$$\Xi = \sum_{k=1}^{\ell} \binom{\ell}{k} \mathcal{O}(\varepsilon^{2k}) \leq \sum_{k=1}^{\ell} \frac{\ell^k}{k!} \mathcal{O}(\varepsilon^{2k}) = \sum_{k=1}^{\ell} \frac{1}{k!} \mathcal{O}(\varepsilon^k) = \mathcal{O}(\varepsilon),$$

which proves (24) for $t = \tau_\ell$.

Now let $\tau_\ell > t$. The previous argument shows:

$$\begin{aligned} \mathcal{T}e^{\int_0^{\tau_\ell} \Delta_{g(\tau)} d\tau} &= (I + \varepsilon \Delta_{g(\tau_\ell)}) (I + \varepsilon \Delta_{\ell-1}) \cdots (I + \varepsilon \Delta_1) + \mathcal{O}(\varepsilon), \\ \mathcal{T}e^{\int_0^t \Delta_{g(\tau)} d\tau} &= (I + \varepsilon \Delta_{g(t)}) (I + \varepsilon \Delta_{\ell-1}) \cdots (I + \varepsilon \Delta_1) + \mathcal{O}(\varepsilon). \end{aligned}$$

Therefore the difference between the two operators is:

$$\|\mathcal{T}e^{\int_0^{\tau_\ell} \Delta_{g(\tau)} d\tau} - \mathcal{T}e^{\int_0^t \Delta_{g(\tau)} d\tau}\| \leq \varepsilon \|\Delta_{g(\tau_\ell)} - \Delta_{g(t)}\| + \mathcal{O}(\varepsilon) \leq C\varepsilon^2 + \mathcal{O}(\varepsilon) = \mathcal{O}(\varepsilon),$$

and so (24) holds for any $0 < t \leq T$. \square

Proof of Theorem 3.1. Recall that each of our diffusion operators $\mathbf{P}_{\varepsilon, i}$ for a fixed i is defined the same as in the standard diffusion maps framework. Hence, by adapting the convergence result from Singer [28], we have that on E_K :

$$\mathbf{P}_{\varepsilon, i} = I + \varepsilon \Delta_i + \mathcal{O}\left(\frac{1}{n^{1/2} \varepsilon^{d/4-1/2}}, \varepsilon^2\right).$$

Let $\ell = \lceil t/\varepsilon \rceil$ and recall our ℓ -step transition operator $\mathbf{P}_\varepsilon^{(\ell)}$ is defined as $\mathbf{P}_\varepsilon^{(\ell)} := \mathbf{P}_{\varepsilon, \ell} \mathbf{P}_{\varepsilon, \ell-1} \cdots \mathbf{P}_{\varepsilon, 1}$. The proof of Lemma 3.3 demonstrates that the error of the product increases by a factor of ε , hence:

$$\mathbf{P}_\varepsilon^{(\ell)} = (I + \varepsilon \Delta_\ell) (I + \varepsilon \Delta_{\ell-1}) \cdots (I + \varepsilon \Delta_1) + \mathcal{O}\left(\frac{1}{n^{1/2} \varepsilon^{d/4+1/2}}, \varepsilon\right).$$

Therefore using Lemma 3.3 we conclude that

$$\mathbf{P}_\varepsilon^{(\lceil t/\varepsilon \rceil)} = \mathcal{T}e^{\int_0^t \Delta_{g(\tau)} d\tau} + \mathcal{O}\left(\frac{1}{n^{1/2} \varepsilon^{d/4+1/2}}, \varepsilon\right),$$

on the set E_K , where K is fixed but arbitrary. The result follows by taking the union and closure $\overline{\bigcup_{K>0} E_K}$, as in [4]. \square

Remark. The connection to heat diffusion can be also considered in terms of infinitesimal generators. For the static case, the product $\mathbf{P}_\epsilon^{t/\epsilon}$ approaches a continuous-time Markov operator P_t , which can be represented in terms of a generator G as $P_t = e^{tG}$ where $G = \Delta$. In the above, we have shown that the $\lceil t/\epsilon \rceil$ -step transition operator for our inhomogeneous Markov chain $\mathbf{P}_\epsilon^{\lceil t/\epsilon \rceil}$ approaches the continuous process $\mathcal{T}e^{\int_0^t \Delta_{g(\tau)} d\tau}$, whose time-dependent infinitesimal generator at time t is $\Delta_{g(t)}$.

4. NUMERICAL EXAMPLE

Suppose that D consists of $n = 10,000$ points sampled uniformly at random from the unit disc in \mathbb{R}^2 . Define the maps $h, v : \mathbb{R}^2 \rightarrow \mathbb{R}^2$ by

$$h(x, y) = (x, y \cdot (1 - \cos \pi x)), \quad \text{and} \quad v(x, y) = (x \cdot (1 - \cos \pi y), y).$$

We refer the images $h(D)$ and $v(D)$ as horizontal and vertical barbells, respectively. In the following, we define a deformation of the $n = 10,000$ points from a horizontal to a vertical barbell over $m = 9$ times. We define $X_1 = h(D)$, $X_5 = D$, and $X_9 = v(D)$. The intermediate sets X_2, X_3, X_4 and X_6, X_7, X_8 are defined by linear interpolation. Specifically, if $X_i = \left\{ x_j^{(i)} \right\}_{j=1}^n$, then

$$x_j^{(i)} = \left(x_j^{(5)} - x_j^{(1)} \right) \cdot \frac{i-1}{4} + x_j^{(1)} \quad \text{and} \quad x_j^{(i)} = \left(x_j^{(9)} - x_j^{(5)} \right) \cdot \frac{i-5}{4} + x_j^{(5)},$$

for $i = 2, 3, 4$ and $i = 6, 7, 8$, respectively. In the first row of Figure 2 the data X_i is plotted for $i = 1, 5, 9$.

From a computational point of view the sequence of data sets (X_1, \dots, X_9) can be stored as an $10,000 \times 2 \times 9$ data tensor corresponding to the 10,000 points in \mathbb{R}^2 measured over the 9 times. Moreover, by fixing the first coordinate of this tensor, we have a 2×9 matrix corresponding to the trajectory of a single point through \mathbb{R}^2 over the 9 times. Note how, as discussed in Section 2.1, even though points were sampled uniformly at time $i = 5$, the deformation of the data manifold creates a nonuniform distribution of points at the other times. In the following, we compare three methods of embedding the data.

First, as a baseline, we compute the diffusion map for each fixed data set X_1, X_5 , and X_9 and plot the first three embedding coordinates ϕ_1, ϕ_2, ϕ_3 in the second row of Figure 2. Second, we define a concatenated data diffusion map based on the concatenation of the data up to time i . That is, at time i we consider the data

$$X_{(i)} := \left\{ \left(x_j^{(1)}, \dots, x_j^{(i)} \right) \right\}_{j=1}^n \subseteq \mathbb{R}^{2i},$$

and construct a diffusion map via equations (2), (3), (4), and (5), where the kernel $\mathbf{K}_{\epsilon, i}(x_j, x_k)$ in equation (2) is replaced by the Gaussian kernel $\mathbf{K}_{\epsilon, i}^{\text{concat}}(x_j, x_k)$ defined by

$$\mathbf{K}_{\epsilon, i}^{\text{concat}}(x_j, x_k) := \exp \left(- \frac{\left\| \left(x_j^{(1)}, \dots, x_j^{(i)} \right) - \left(x_k^{(1)}, \dots, x_k^{(i)} \right) \right\|_{\ell^2(\mathbb{R}^{2i})}^2}{\epsilon} \right).$$

The first three coordinates $\zeta_1, \zeta_2, \zeta_3$ of the concatenated data diffusion map are plotted in the third row of Figure 2. Finally, for $\{X_i\}_{i=1}^1, \{X_i\}_{i=1}^5$, and $\{X_i\}_{i=1}^9$ we computed the time coupled diffusion map and plot the first three coordinates ψ_1, ψ_2, ψ_3 in the fourth row of Figure 2. We would like to draw the reader's attention to the difference between the concatenated data diffusion map and the time coupled diffusion map at time $i = 9$. To facilitate visualization, we have plotted the first two coordinates of these embeddings in Figure 3.

Observe that each point x_j in the data $\left\{ x_j^{(i)} \right\}_{j=1}^n$, $i = 1, \dots, 9$ can be assigned one for four classes:

(right-up), (right-down), (left-up), or (left-down),

corresponding to side (left or right) that the point resides in the horizontal barbell at $i = 1$, and the side (up or down) that the point resides in the vertical barbell at time $i = 9$. Each of the four

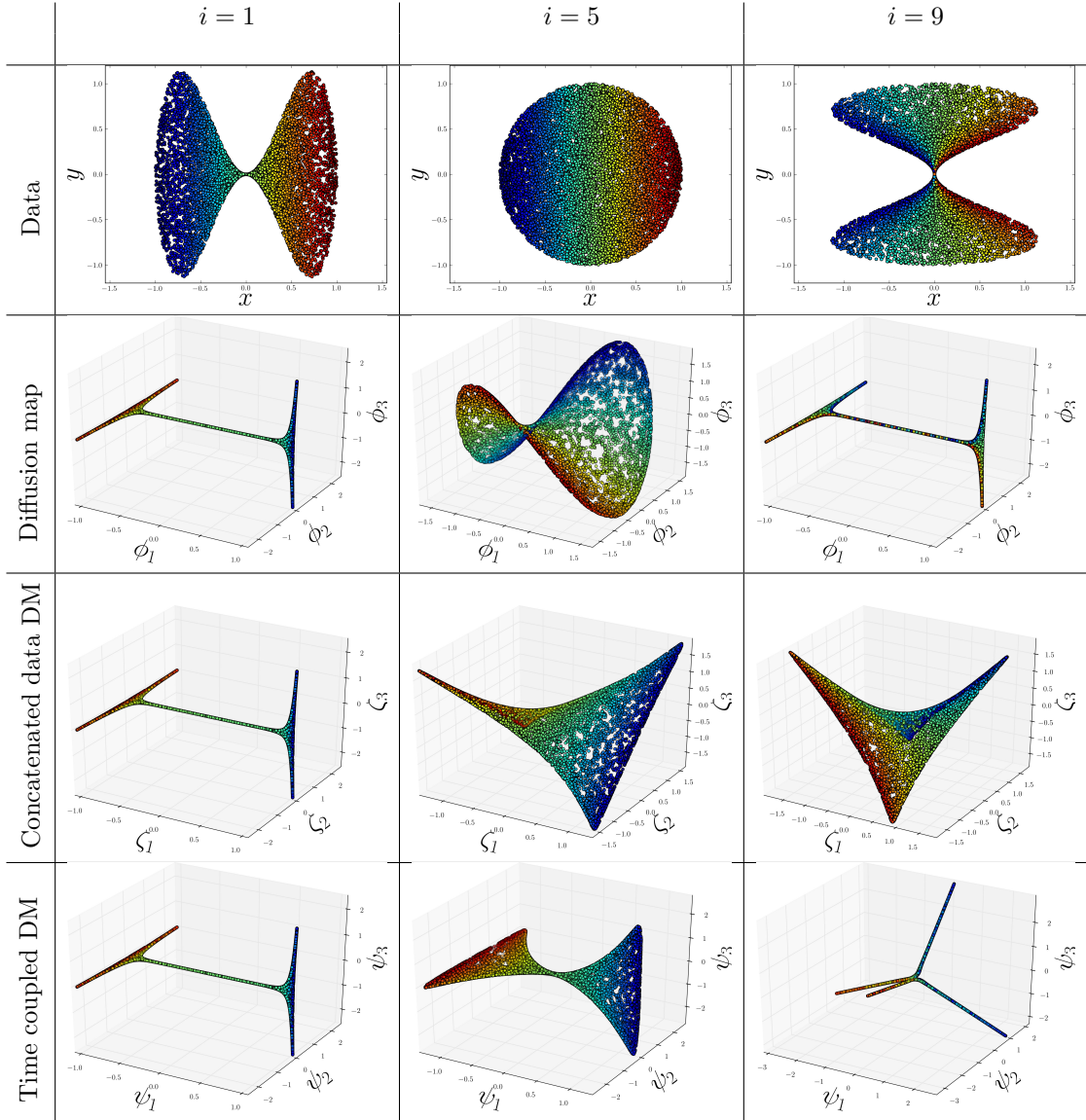


FIGURE 2. In the first row, the data sets X_i are plotted for times $i = 1, 5, 9$; in the second row, the first three coordinates of the diffusion map of the fixed sets X_1, X_5 , and X_9 are plotted; in the third row, the first three coordinates for the concatenated data diffusion map (as described in Section 4) for the sequences of data sets $\{X_i\}_{i=1}^1$, $\{X_i\}_{i=1}^5$, and $\{X_i\}_{i=1}^9$ are plotted; finally, in the fourth row, the time coupled diffusion map for the sequences of data sets $\{X_i\}_{i=1}^1$, $\{X_i\}_{i=1}^5$, and $\{X_i\}_{i=1}^9$ are plotted. A consistent color map is used across all plots.

lines in the time coupled diffusion map embedding correspond to one of these four classes. On the other hand, we interpret the concatenated data diffusion map by observing that the kernel $\mathbf{K}_{\varepsilon, i}^{\text{concat}}(x_j, x_k)$ can also be written

$$\mathbf{K}_{\varepsilon, i}^{\text{concat}}(x_j, x_k) = \exp\left(-\frac{\sum_{l=1}^i \|x_j^{(l)} - x_k^{(l)}\|_{\ell^2(\mathbb{R}^2)}^2}{\varepsilon}\right) = \prod_{l=1}^i \exp\left(-\frac{\|x_j^{(l)} - x_k^{(l)}\|_{\ell^2(\mathbb{R}^2)}^2}{\varepsilon}\right).$$

Thus, concatenating the available data is equivalent to either averaging (up to a constant) the square distances for the available times, or multiplying the Gaussian kernels pointwise for the

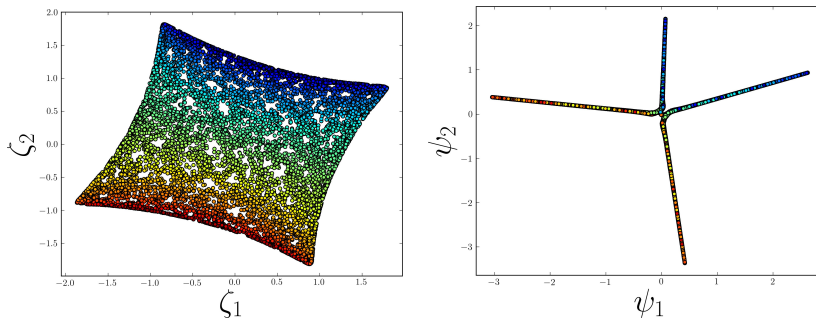


FIGURE 3. For time $i = 9$ the first two coordinates of the concatenated data DM (left) and time coupled DM (right) are plotted.

available times. The resulting concatenated data diffusion map encodes the fact that on average the points are spread out over the disc; the only indication of the existence of the barbells at times $i = 1$ and $i = 9$ are the corners in the embedding. In contrast, the time coupled diffusion map embedding clearly captures the two barbell events: the four lines in this embedding represent the four classes in the data induced by the barbell events at times $i = 1$ and $i = 9$. Moreover, this numerical example demonstrates that the time coupled diffusion map embedding aggregates information over time. Indeed, the two barbell events are temporally disjoint and thus no single temporal slice of the data is sufficient to recover the four classes in the data. This temporal disjointness is reflected in the standard diffusion map embeddings in row two of Figure 2. In summary, the numerical results provide an example where averaging square distances over time, or equivalently multiplying Gaussian kernels pointwise over time, is insufficient to capture geometric events in the evolution of the data; instead, by viewing the data as an evolving manifold and approximating heat flow on the manifold via the product of diffusion operators, we are able to define an embedding which provides a concise description of the structures which occur in the evolution of the data.

5. CONTINUOUS TIME COUPLED DIFFUSION MAP

Theorem 3.1 approximates the operator $T_Z^{(t)} : L^2(\mathcal{M}) \rightarrow L^2(\mathcal{M})$, defined in (20), with the discrete inhomogeneous Markov chain $\mathbf{P}_\varepsilon^{\lceil t/\varepsilon \rceil}$. The inhomogeneous chain $\mathbf{P}_\varepsilon^{\lceil t/\varepsilon \rceil}$ is the foundation of the time coupled diffusion distance, and after the normalization in (9) the singular value decomposition can be used to construct the corresponding time coupled diffusion map (12). In this section we further investigate the connection between the heat kernel Z and the time coupled diffusion map through the continuous operator $T_Z^{(t)}$.

Recall the diffusion operator $T_Z^{(t)} f(x) = \int_{\mathcal{M}} Z(x, t; y, 0) f(y) dV(y, 0)$ introduced in Section 3. If f is an initial distribution over \mathcal{M} , the operator $T_Z^{(t)}$ diffuses f forward in time over the changing manifold geometry, up to time $\tau = t$. The adjoint of this operator is $(T_Z^{(t)})^* : L^2(\mathcal{M}) \rightarrow L^2(\mathcal{M})$,

$$(T_Z^{(t)})^* f(x) = \int_{\mathcal{M}} Z(y, t; x, 0) f(y) dV(y, t).$$

It follows from (18) that the operator $(T_Z^{(t)})^*$ maps a probability distribution over $(\mathcal{M}, g(t))$ backwards in time to a probability distribution over $(\mathcal{M}, g(0))$. Indeed, if f is a probability density function, then $(T_Z^{(t)})^* f$ is its posterior probability distribution as in Section 2. In the continuous setting, the analysis is performed over the manifold $(\mathcal{M}, g(\cdot))$, and all integration is performed with respect to the Riemannian volume on the manifold similar to the approach in [22, 21, 20]. In the continuous case, the stationary distribution is constant and the normalization in (9) is therefore unnecessary. Moreover, the operator $T_Z^{(t)}$ is bi-stochastic in the sense that the

constant function is an eigenfunction of both $T_Z^{(t)}$ and $(T_Z^{(t)})^*$. Indeed, in Lemma 3.2 we showed that $T_Z^{(t)}$ can be written as the limit of a product – with an increasing number of terms – of self-adjoint operators, which each have the constant eigenfunction. Therefore, the continuous analog of the discrete diffusion distance (7) is the diffusion distance

$$D^{(t)}(x, y)^2 = \int_{\mathcal{M}} (Z(x, t; w, 0) - Z(y, t; w, 0))^2 dV(w, 0),$$

or equivalently,

$$D^{(t)}(x, y) = \left\| \left(T_Z^{(t)} \right)^* \delta_x - \left(T_Z^{(t)} \right)^* \delta_y \right\|_{L^2(\mathcal{M})},$$

where δ_x is the Dirac distribution centered at $x \in \mathcal{M}$ (compare to (7)). Since the “row” sums of $Z(x, t, y, 0)$ are 1 (see (18)), and the manifold \mathcal{M} is compact:

$$\int_{\mathcal{M}} \int_{\mathcal{M}} Z(x, t; y, 0) dV(y, 0) dV(x, t) < \infty$$

Therefore, the operator $T_Z^{(t)} f(x) = \int_{\mathcal{M}} Z(x, t; y, 0) f(y) dV(y, 0)$ is compact, see for example [29]. Similarly, the operator $(T_Z^{(t)})^*$ is compact, and thus $T_Z^{(t)} (T_Z^{(t)})^*$ is compact, since it is the composition of two compact operators. Moreover, since $T_Z^{(t)} (T_Z^{(t)})^*$ is also self-adjoint, by the spectral theorem $T_Z^{(t)} (T_Z^{(t)})^*$ has an eigendecomposition, and similarly, $(T_Z^{(t)})^* T_Z^{(t)}$ has an eigendecomposition. Therefore, analogous to the discrete decomposition (10), $T_Z^{(t)}$ has a singular value decomposition.

$$T_Z^{(t)} f(x) = \sum_{k \geq 0} \sigma_k^{(t)} \langle f, \varphi_k^{(t)} \rangle \psi_k^{(t)}(x),$$

where $\varphi_k^{(t)} \in L^2(\mathcal{M})$ is a right singular function of $T_Z^{(t)}$ (an eigenfunction of $(T_Z^{(t)})^* T_Z^{(t)}$), $\psi_k^{(t)} \in L^2(\mathcal{M})$ is a left singular function of $T_Z^{(t)}$ (an eigenfunction of $T_Z^{(t)} (T_Z^{(t)})^*$), and $\{\sigma_k^{(t)}\}_{k \geq 0}$ are the corresponding singular values (the square root of the eigenvalues of $(T_Z^{(t)})^* T_Z^{(t)}$, or equivalently the square root of the eigenvalues of $T_Z^{(t)} (T_Z^{(t)})^*$ since these operators share the same spectrum). However, recall that in the discrete case, we must take into account the stationary distribution of the Markov chain using the normalization in (9), since the discrete operator $\mathbf{P}_\varepsilon^{(t)}$ is not in general bi-stochastic. In the continuous setting left singular functions are used to define the time coupled diffusion map (12), written here as:

$$\Psi^{(t)}(x) = \left(\sigma_k^{(t)} \psi_k^{(t)}(x) \right)_{k \geq 1}.$$

where the index k starts at 1 because the 0th left singular function is constant.

We remark that the operator $T_Z^{(t)} (T_Z^{(t)})^*$ can be written as an integral operator

$$(26) \quad T_Z^{(t)} (T_Z^{(t)})^* f(x) = \int_{\mathcal{M}} K_Z^b(x, y; t) f(y) dV(y, t),$$

where

$$K_Z^b(x, y; t) = \int_{\mathcal{M}} Z(x, t; w, 0) Z(y, t; w, 0) dV(w, 0).$$

We refer to $K_Z^b(x, y; t)$ as the backwards kernel since it is integrated against functions on $(M, g(t))$, i.e., integrated against functions with respect to the Riemannian volume at the end of the time interval $[0, t]$. Similarly, the operator $(T_Z^{(t)})^* T_Z^{(t)}$ has integral representation

$$(T_Z^{(t)})^* T_Z^{(t)} f(x) = \int_{\mathcal{M}} K_Z^f(x, y; t) f(y) dV(y, 0),$$

where

$$K_Z^f(x, y; t) = \int_{\mathcal{M}} Z(w, t; x, 0)Z(w, t; y, 0) dV(w, t).$$

We refer to K_Z^f as the forward kernel since it is integrated against functions on $(\mathcal{M}, g(0))$. The kernels K_Z^b and K_Z^f can be interpreted as analogous to the matrices $\mathbf{A}^{(t)}(\mathbf{A}^{(t)})^\top$ and $(\mathbf{A}^{(t)})^\top \mathbf{A}^{(t)}$ from the discrete case, whose eigenfunctions are the left and right singular vectors of $\mathbf{A}^{(t)}$, respectively.

Since the time coupled diffusion map is based on the SVD of $T_Z^{(t)}$ diffusing $\varphi_k^{(t)}$ forward in time results in $\sigma_k^{(t)}\psi_k^{(t)}$, and conversely the backward propagation of $\psi_k^{(t)}$ leads to $\sigma_k^{(t)}\varphi_k^{(t)}$; specifically $T_Z^{(t)}\varphi_k^{(t)} = \sigma_k^{(t)}\psi_k^{(t)}$ and $(T_Z^{(t)})^*\psi_k^{(t)} = \sigma_k^{(t)}\varphi_k^{(t)}$. If we define,

$$\tilde{\Phi}^{(t)}(x) = \left(\varphi_k^{(t)}(x)\right)_{k \geq 1}$$

and set $T_Z^{(t)}\tilde{\Phi}^{(t)}(x) = (T_Z^{(t)}\varphi_k^{(t)}(x))_{k \geq 1}$, then this observation leads to:

$$D^{(t)}(x, y) = \left\| \left(T_Z^{(t)}\right)^* \delta_x - \left(T_Z^{(t)}\right)^* \delta_y \right\|_{L^2(\mathcal{M})} = \left\| \Psi^{(t)}(x) - \Psi^{(t)}(y) \right\|_{\ell^2} = \left\| T_Z^{(t)}\tilde{\Phi}^{(t)}(x) - T_Z^{(t)}\tilde{\Phi}^{(t)}(y) \right\|_{\ell^2}.$$

We see that the difference in posterior distributions of δ_x and δ_y is equivalent to the difference between the diffused distributions of $\tilde{\Phi}^{(t)}(x)$ and $\tilde{\Phi}^{(t)}(y)$; these equivalent distances are, in turn, equal to the Euclidean distance between points under the time coupled diffusion map $\Psi^{(t)}$.

6. CONCLUSION

We have introduced the notion of time coupled diffusion maps as a method of summarizing evolving data via an embedding into Euclidean space. In particular, we have introduced a method of modeling evolving data as samples from a manifold with a time-dependent metric. We show that the constructed time inhomogeneous Markov chain approximates heat diffusion over a manifold $(\mathcal{M}, g(\cdot))$ with a smoothly varying family of metrics $g(\tau)$. In the context of manifold learning, these operators and resulting embeddings are related to the heat kernel of $\partial_t u = \Delta_{g(t)} u$, which provides geometric and probabilistic interpretations. Numerical experiments indicate that the map encodes aggregate geometrical information over arbitrarily long time scales, and thus summarizes the geometry of a sequence of datasets in a useful way.

These results open new directions related to diffusion based manifold learning, and in particular the use of inhomogeneous Markov chains and asymmetric diffusion semi-groups to understand data geometry. Early results on single cell data [11] show the usefulness of this type of diffusion process in biology, but further numerical and theoretical study is needed. Understanding precisely the nature of the geometrical information encoded by the time coupled diffusion map (extending [21, 22]), would give theoretical insight and could lead to further developments. More immediately, the results contained here provide a theoretical foundation for understanding dynamic data that can be modeled as a time varying manifold.

7. ACKNOWLEDGEMENTS

N.M. was a participant in the 2013 Research Experience for Undergraduates (REU) at Cornell University under the supervision of M.H. During the REU program both were supported by the National Science Foundation grant number NSF-1156350. This paper is the result of work started during the REU. M.H. was supported by the European Research Council (ERC) grant InvariantClass 320959 while writing the first version of the paper. He is currently supported by the Alfred P. Sloan Fellowship (grant number FG-2016-6607), the DARPA Young Faculty Award (grant number D16AP00117), and the NSF (grant number 1620216).

Both authors would like to thank Ronald Coifman for numerous insightful conversations, and the reviewers for their comments which improved the manuscript.

REFERENCES

- [1] M. Belkin, Problems of learning on manifolds, Ph.D. thesis, University of Chicago (2003).
- [2] S. Lafon, Diffusion maps and geometric harmonics, Ph.D. thesis, Yale University (2004).
- [3] M. Belkin, P. Niyogi, Towards a theoretical foundation for Laplacian-based manifold methods, *Journal of Computer and System Sciences* 74 (8) (2008) 1289–1308.
- [4] R. R. Coifman, S. Lafon, Diffusion maps, *Applied and Computational Harmonic Analysis* 21 (1) (2006) 5 – 30.
- [5] A. Singer, From graph to manifold Laplacian: The convergence rate, *Applied and Computational Harmonic Analysis* 21 (1) (2006) 128–134.
- [6] A. Singer, H. Wu, Vector diffusion maps and the connection laplacian, *Communications on Pure and Applied Mathematics* 65 (8) (2012) 1067–1144.
- [7] G. Wolf, A. Averbuch, Linear-projection diffusion on smooth euclidean submanifolds, *Applied and Computational Harmonic Analysis* 34 (1) (2013) 1–14.
- [8] T. Berry, T. Sauer, Local kernels and the geometric structure of data, *Applied and Computational Harmonic Analysis* (2015) In press.
- [9] R. Talmon, I. Cohen, S. Gannot, R. Coifman, Diffusion maps for signal processing: A deeper look at manifold-learning techniques based on kernels and graphs, *Signal Processing Magazine, IEEE* 30 (4) (2013) 75–86. doi:10.1109/MSP.2013.2250353.
- [10] A. D. Szlam, M. Maggioni, R. R. Coifman, Regularization on graphs with function-adapted diffusion processes, *Journal of Machine Learning Research* 9 (2008) 1711–1739.
URL <http://jmlr.org/papers/volume9/szlam08a/szlam08a.pdf>
- [11] T. Welp, G. Wolf, M. Hirn, S. Krishnaswamy, A diffusion-based condensation process for multiscale analysis of single cell data, in: *ICML Workshop Computational Biology*, New York, NY, 2016, pp. 1–5, 5 pages.
- [12] B. Wang, J. Jiang, W. Wang, Z.-H. Zhou, Z. Tu, Unsupervised metric fusion by cross diffusion, in: *Computer Vision and Pattern Recognition (CVPR), 2012 IEEE Conference on*, 2012, pp. 2997–3004. doi:10.1109/CVPR.2012.6248029.
- [13] R. R. Coifman, M. J. Hirn, Diffusion maps for changing data, *Applied and Computational Harmonic Analysis* 36 (1) (2014) 79 – 107. doi:http://dx.doi.org/10.1016/j.acha.2013.03.001.
URL <http://www.sciencedirect.com/science/article/pii/S1063520313000225>
- [14] R. R. Lederman, R. Talmon, Common manifold learning using alternating-diffusion, Tech. rep., Yale (2014).
- [15] R. R. Lederman, R. Talmon, H. t. Wu, Y. L. Lo, R. R. Coifman, Alternating diffusion for common manifold learning with application to sleep stage assessment, in: *2015 IEEE International Conference on Acoustics, Speech and Signal Processing (ICASSP)*, 2015, pp. 5758–5762. doi:10.1109/ICASSP.2015.7179075.
- [16] O. Lindenbaum, A. Yeredor, M. Salhov, A. Averbuch, Multiview diffusion maps, arXiv:1508.05550 (2015).
- [17] R. Talmon, H.-t. Wu, Latent common manifold learning with alternating diffusion: analysis and applications, ArXiv e-prints arXiv:1602.00078.
- [18] R. Banisch, P. Koltai, Understanding the geometry of transport: Diffusion maps for lagrangian trajectory data unravel coherent sets, *Chaos* 27 (2017) 035804, arXiv:1603.04709.
- [19] T. Berry, J. Harlim, Variable bandwidth diffusion kernels, *Applied and Computational Harmonic Analysis* 1 (0) (2015) –. doi:http://dx.doi.org/10.1016/j.acha.2015.01.001.
URL <http://www.sciencedirect.com/science/article/pii/S1063520315000020>
- [20] P. Bérard, G. Besson, S. Gallot, Embedding Riemannian manifolds by their heat kernel, *Geometric and Functional Analysis* 4 (4) (1994) 373–398.
- [21] H. Abdallah, Processus de diffusion sur un flot de variétés Riemanniennes, Ph.D. thesis, L’Universite de Grenoble (2010).
- [22] H. Abdallah, Embedding Riemannian manifolds via their eigenfunctions and their heat kernel, *Bulletin of the Korean Mathematical Society* 49 (5) (2012) 939–947.
- [23] H. Rutishauser, Computational aspects of f. l. bauer’s simultaneous iteration method, *Numer. Math.* 13 (1) (1969) 4–13. doi:10.1007/BF02165269.
URL <http://dx.doi.org/10.1007/BF02165269>
- [24] C. M. Guenther, The fundamental solution on manifolds with time-dependent metrics, *The Journal of Geometric Analysis* 12 (3) (2002) 425–436. doi:10.1007/BF02922048.
- [25] B. Chow, S.-C. Chu, D. Glickenstein, C. Guenther, J. Isenber, T. Ivey, D. Knopf, P. Lu, F. Luo, L. Ni, *The Ricci Flow: Techniques and Applications Part III: Geometric-Analytic Aspects*, Vol. 163, AMS, 2008.
- [26] P.-L. Giscard, K. Lui, S. J. Thwaite, D. Jaksch, An exact formulation of the time-ordered exponential using path-sums, ArXiv e-prints arXiv:1410.6637.
- [27] S. Mousazadeh, I. Cohen, Out-of-sample extension of band-limited functions on homogeneous manifolds using diffusion maps, *Signal Processing* 108 (0) (2015) 521 – 529. doi:http://dx.doi.org/10.1016/j.sigpro.2014.10.024.
URL <http://www.sciencedirect.com/science/article/pii/S0165168414004885>
- [28] A. Singer, From graph to manifold laplacian: The convergence rate, *Applied and Computational Harmonic Analysis* 21 (1) (2006) 128 – 134, special Issue: Diffusion Maps and Wavelets. doi:http://dx.doi.org/10.1016/j.acha.2006.03.004.
URL <http://www.sciencedirect.com/science/article/pii/S1063520306000510>
- [29] M. Pedersen, *Functional analysis in applied mathematics and engineering*, Chapman & Hall : CRC Press, 2000.

APPENDIX A. DIFFUSION GEOMETRY FROM MARKOV KERNELS

We show that the operator $\mathbf{A}^{(t)}$, defined in Section 2, line (9), has operator norm one and that $\pi_{(t)}^{1/2}$, the square root of its stationary distribution, is an eigenvector with eigenvalue one. We do so by following [2] and developing a diffusion geometry framework starting from a Markov kernel.

Suppose that (\mathcal{X}, dx) is a measure space equipped with a Markov kernel $p(x, y)$. Moreover, we assume the kernel $p(x, y)$ nonnegative and has the conservation property

$$\int_{\mathcal{X}} p(x, y) dy = 1 \quad \text{for all } x \in \mathcal{X}.$$

The kernel $p(x, y)$ induces a Markov operator P^* from $L^2(\mathcal{X})$ to itself defined by

$$(P^*f)(x) = \int_{\mathcal{X}} p(y, x)f(y) dy \quad \text{for all } x \in \mathcal{X}.$$

The notation P^* has been used to bring attention to the fact that P^* is the adjoint of the operator P defined as:

$$(Pf)(x) = \int_{\mathcal{X}} p(x, y)f(y) dy.$$

We assume that P^* has a unique strictly positive stationary distribution $v^2(x)$, that is to say,

$$(P^*v^2)(x) = \int_{\mathcal{X}} p(y, x)v^2(y) dy = v^2(x) \quad \text{for all } x \in \mathcal{X}.$$

For example, if \mathcal{X} is a finite set with the counting measure (as in Section 2), it would suffice to assume that the Markov chain is irreducible and positive recurrent. By the function $v(x)$, we denote the positive pointwise square root of $v^2(x)$. We define an operator $A : L^2(\mathcal{X}) \rightarrow L^2(\mathcal{X})$ by

$$(27) \quad (Af)(x) = \int_{\mathcal{X}} \frac{v(x)p(x, y)}{v(y)} f(y) dy = \int_{\mathcal{X}} a(x, y)d(y) dy \quad \text{for all } x \in \mathcal{X}.$$

Here the kernel $a(x, y) = v(x)p(x, y)/v(y)$. We refer to A as an averaging or diffusion operator and show it has several nice properties.

Lemma A.1. *The operator norm $\|A\| = 1$, and the norm is achieved by the function $v(x)$.*

Remark. *Taking $A = \mathbf{A}^{(t)}$ establishes the claim from the beginning of the appendix, which was originally stated after line (9) in Section 2.*

Proof. First we evaluate $(Av)(x)$ to check the second part of the assertion and establish a lower bound on the operator norm:

$$(Av)(x) = \int_{\mathcal{X}} v(x)p(x, y) \frac{v(y)}{v(y)} dy = v(x) \int_{\mathcal{X}} p(x, y) dy = v(x),$$

using the Markov property of the kernel. To establish that 1 is an upper bound on the operator norm we show that $\langle Af, Af \rangle \leq \|f\|^2$. First, observe that by Cauchy-Schwartz,

$$(28) \quad \left| \int_{\mathcal{X}} \frac{v^2(x)p(x, y)f(y)}{v(y)} dy \right| \leq \left(\int_{\mathcal{X}} v^2(x)p(x, y) dy \right)^{1/2} \left(\int_{\mathcal{X}} \frac{v^2(x)p(x, y)}{v^2(y)} f^2(y) dy \right)^{1/2},$$

$$= v(x) \cdot \left(\int_{\mathcal{X}} \frac{v^2(x)p(x, y)}{v^2(y)} f^2(y) dy \right)^{1/2}.$$

Now starting with $\langle Af, Af \rangle$ we multiply and divide by $v^2(x)$ yielding:

$$\langle Af, Af \rangle = \int_{\mathcal{X}} \frac{1}{v^2(x)} \int_{\mathcal{X}} \frac{v(x)^2 p(x, y) f(y)}{v(y)} dy \int_{\mathcal{X}} \frac{v(x)^2 p(x, z) f(z)}{v(z)} dz dx.$$

By applying the inequality (28) we see that,

$$\langle Af, Af \rangle \leq \int_{\mathcal{X}} \left(\int_{\mathcal{X}} \frac{v^2(x)p(x, y)}{v^2(y)} f^2(y) dy \right)^{1/2} \left(\int_{\mathcal{X}} \frac{v^2(x)p(x, z)}{v^2(z)} f^2(z) dy \right)^{1/2} dx.$$

Applying Cauchy-Schwartz again,

$$\langle Af, Af \rangle \leq \left(\int_{\mathcal{X}} \int_{\mathcal{X}} \frac{v^2(x)p(x,y)}{v^2(y)} f^2(y) dy dx \right)^{1/2} \left(\int_{\mathcal{X}} \int_{\mathcal{X}} \frac{v^2(x)p(x,z)}{v^2(z)} f^2(z) dz dx \right)^{1/2}.$$

Finally, using the fact that $v^2(x)$ is the stationary distribution shows that:

$$\langle Af, Af \rangle \leq \left(\int_{\mathcal{X}} f(y)^2 dy \right)^{1/2} \left(\int_{\mathcal{X}} f(z)^2 dz \right)^{1/2} = \|f\|^2,$$

as was to be shown. □

APPENDIX B. UNIFORM BOUNDEDNESS OF $\Delta_{g(\tau)}$ ON E_K

We prove that the family of operators $\{\Delta_{g(\tau)}\}_{0 \leq \tau \leq T}$ is uniformly bounded on $E_K \subset L^2(\mathcal{M})$, where

$$E_K = \text{Span}\{\phi_l : 0 \leq l \leq K\},$$

and ϕ_l is the l^{th} eigenfunction of $\Delta_{g(0)}$ with eigenvalue λ_l , ordered so that $0 = \lambda_0 < \lambda_1 \leq \dots \leq \lambda_K$.

To simplify notation, set $\Delta_\tau = \Delta_{g(\tau)} : E_K \rightarrow L^2(\mathcal{M})$, and consider the function $\alpha(\tau) = \|\Delta_\tau\|$. If $\alpha(\tau)$ is a continuous function in τ , then $\alpha(\tau)$ is uniformly bounded on $[0, T]$ since $\alpha(0) = \lambda_K < \infty$ and $[0, T]$ is compact. It thus remains to show that $\alpha(\tau)$ is a continuous function.

Let $\Delta_\tau^* : L^2(\mathcal{M}) \rightarrow E_K$ be the adjoint of Δ_τ . It suffices to show that $\beta(\tau) = \|\Delta_\tau^* \Delta_\tau\|$ is a continuous function in τ , since $\|\Delta_\tau^* \Delta_\tau\| = \|\Delta_\tau\|^2$. We have $\Delta_\tau^* \Delta_\tau : E_K \rightarrow E_K$, and so the operator $\Delta_\tau^* \Delta_\tau$ can be represented by the $(K+1) \times (K+1)$ matrix M_τ , defined through:

$$\Delta_\tau^* \Delta_\tau \phi_j = \sum_{i=0}^{K+1} (M_\tau)_{ij} \phi_i.$$

Recalling that the metric tensor $g(\tau)$ varies smoothly in τ , it follows that the entries of M_τ are continuous in τ since in local coordinates:

$$\Delta_\tau f = \frac{1}{\sqrt{|g(\tau)|}} \partial_i \left(\sqrt{|g(\tau)|} g(\tau)^{ij} \partial_j f \right),$$

where $|g(\tau)|$ is the determinant of $g(\tau)$ in the local chart, $g(\tau)^{ij}$ are the entries of the inverse of the metric tensor, and the Einstein summation convention is used. But then the eigenvalues of M_τ vary continuously in τ , and in particular the operator norm of M_τ is a continuous function of τ .

DEPARTMENT OF MATHEMATICS, YALE UNIVERSITY, NEW HAVEN, CT 06511, USA
E-mail address: `nicholas.marshall@yale.edu`

DEPARTMENT OF COMPUTATIONAL MATHEMATICS, SCIENCE & ENGINEERING AND DEPARTMENT OF MATHEMATICS,
 MICHIGAN STATE UNIVERSITY, EAST LANSING, MI 48824, USA
E-mail address: `mhirn@msu.edu`